JOURNAL OF QUATERNARY SCIENCE (2018) **33**(6) 662–676 ISSN 0267-8179. DOI: 10.1002/jqs.3043

JQS Journal of Quaternary Science QRA Quaternary Research Association

A new multi-proxy investigation of Late Quaternary palaeoenvironments along the north-western Barents Sea (Storfjorden Trough Mouth Fan)

ROMANA MELIS,[1]* KATIA CARBONARA,[2] GIULIANA VILLA,[2] CATERINA MORIGI,[3,4] MARÍA A. BÁRCENA,[5] GIOVANNA GIORGETTI,[6] ANDREA CABURLOTTO,[7] MICHELE REBESCO[7] and RENATA G. LUCCHI[7]

[1]Department of Mathematics and Geosciences, University of Trieste, Trieste, Italy
[2]Department of Chemistry, Life Sciences and Environmental Sustainability, University of Parma, Parma, Italy
[3]Department of Earth Sciences, University of Pisa, Pisa, Italy
[4]GEUS (Geological Survey of Denmark and Greenland), Copenhagen, Denmark
[5]Department of Geology, University of Salamanca, Salamanca, Spain
[6]Department of Physical Sciences, Earth and Environment, University of Siena, Siena, Italy
[7]OGS (Istituto Nazionale di Oceanografia e di Geofisica Sperimentale), Sgonico, Italy

Received 29 November 2016; Revised 4 April 2018; Accepted 17 April 2018

ABSTRACT: A new integrated micropalaeontological study on planktonic and benthic foraminifera, calcareous nannofossils and diatoms was performed on three sediment cores from the Storfjorden Trough Mouth Fan to reconstruct the Late Quaternary palaeoenvironmental and climatic history. Two main intervals were discussed: the last deglaciation (16.2–11.7 ka BP) and the Holocene. The age model relies on palaeomagnetic parameters together with 10 radiocarbon dates. Deglacial sediments had largely diluted the biogenic content which was scarce and poorly preserved. The first occurrence of *Cibicidoides wuellerstorfi* (benthic foraminifer), together with *Turborotalita quinqueloba* (planktonic foraminifer) and *Coscinodiscus* spp. (diatoms) at 11.3 ka BP followed the end of the Younger Dryas cold event and marked the beginning of the early Holocene warm period. Diatoms and planktonic foraminifers indicated a warming of the surface water from 10.5 to 9.2 ka BP, identifying the Holocene Thermal Maximum event. Bottom water fauna registered these warming conditions less clearly. Cooling events were identified during the Holocene, in particular the 8.2 ka BP event and the Neoglacial between 3.2 and 2 ka BP, as shown by the presence of cold-water taxa such as *Gephyrocapsa muellerae* (nannoplankton) and *Neogloboquadrina pachyderma* (planktonic foraminifer). These events were influenced by sea ice extent, cold or relatively warm current influxes. Copyright © 2018 John Wiley & Sons, Ltd.

KEYWORDS: arctic; last deglaciation; microfossils; palaeoclimate; palaeoenvironments.

Introduction

The continental margin of the Barents Sea around the Svalbard Archipelago (76–80°N) has been studied over the last decade to reconstruct the palaeoceanographic variations which occurred during the last 10–30 ka BP (Ślubowska *et al.*, 2005; Rasmussen *et al.*, 2007; Ślubowska-Woldengen *et al.*, 2007, 2008; Risebrobakken *et al.*, 2011; Werner *et al.*, 2013, 2016; Aagaard-Sørensen *et al.*, 2014; Groot *et al.*, 2014; Chauhan *et al.*, 2016). This time span witnessed the most recent global climatic changes, including the Last Glacial Maximum (LGM), the last deglaciation, characterized by several climatic inversions (Heinrich event H1, the Bølling–Allerød, the Younger Dryas, etc.) and the climatically dynamic Holocene.

The north-western continental margin of the Barents Sea, located on the eastern side of the Fram Strait (Fig. 1A,B), represents one of two gateways for the flux of warm water from middle latitudes to the Arctic Ocean (Schauer *et al.*, 2004). The influx of the relative warm and saline Atlantic Water (AW) towards the Arctic Ocean plays a very important role on the climatic conditions of the Arctic environments. The strength of the warm AW influx into the Arctic Seas varied considerably over time (Rahmstorf, 2002; Rasmussen *et al.*, 2007, 2014; Ślubowska-Woldengen *et al.*, 2007, 2008; Risebrobakken *et al.*, 2011; Klitgaard Kristensen et al., 2013; Werner *et al.*, 2013). In this respect, the north-western Barents Sea margin represents a key area for the study of the palaeoceanographic and palaeoenvironmental conditions which occurred during the LGM and the last deglaciation.

The potential for microfossils as palaeoenvironmental proxies in the Nordic Seas has been outlined by several authors (e.g. Gard and Backman, 1990; Baumann and Matthiessen, 1992; Rasmussen *et al.*, 2007; Ślubowska-Woldengen *et al.*, 2007, 2008; Groot *et al.*, 2014; Rasmussen *et al.*, 2014; Rasmussen and Thomsen, 2015; Carbonara *et al.*, 2016). Most of these studies focused on the continental shelf area and the northern and western slope of Svalbard, while the sector in front of the Storfjorden Trough remains less studied. This area is of particular interest in the study of the last deglaciation as the relatively small size of the Storfjorden glacial system makes it very sensitive to small climatic variations, even though its size is sufficient to be representative of this area (Pedrosa *et al.*, 2011). In this study we present new data from an integrated micropalaeontological study on three sediment cores collected on the middle slope of the Storfjorden Trough Mouth Fan (TMF), south of Svalbard (Fig. 1A,B), aiming to investigate the palaeoenvironmental and palaeoclimatic conditions of the study area after the LGM. The integrated use of several taxonomic groups is intended to determine whether they univocally respond to the same climate forcing events

*Correspondence: Romana Melis, as above.
E-mail: melis@units.it (r. melis)

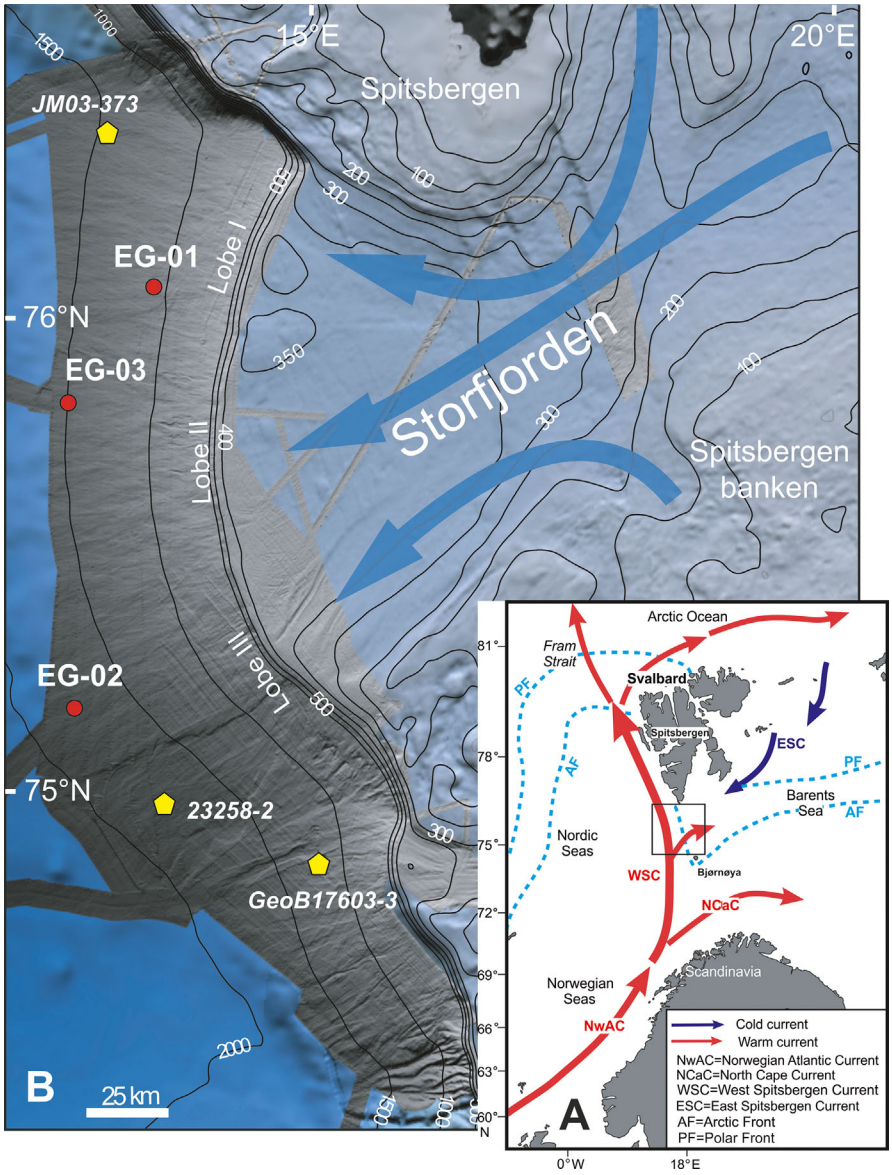

Figure 1. (A) Location of the study area and oceanographic circulation in the north-western Barents Sea (Arctic) (modified after Ślubowska-Woldengen *et al.*, 2008). The black box indicates the location of the study area. (B) Bathymetry of the studied area and core location. The greyscale shaded relief bathymetry derives from the merged high-resolution surveys carried out during the SVAIS and EGLACOM cruises (modified after Pedrosa *et al.*, 2011). Red dots indicate the EGLACOM (EG-) core location. Yellow symbols indicate the location of the cores JM03-373 (Rasmussen *et al.*, 2007), 23258-2 (Sarnthein *et al.*, 2003) and GeoB17603-3 (Carbonara *et al.*, 2016) discussed in the text. Blue arrows represent the direction of the main palaeo ice-streams of Storfjorden trough during the Last Glacial Maximum (LGM) (from Lucchi *et al.*, 2013).

(e.g. Dolven *et al.*, 2002; Risebrobakken *et al.*, 2011 and discussion therein). The results from planktonic foraminifera, calcareous nannofossils and diatoms, as proxies for surface water conditions, were compared with the results from benthic foraminifera as indicators of bottom water conditions. The palaeontological investigation was also integrated with the results from previously published sedimentological and palaeomagnetic studies (Sagnotti *et al.*, 2011; Lucchi *et al.*, 2013).

Regional and oceanographic settings

The Storfjorden TMF depositional system is a NE–SW orientated glacigenic complex located south of the Svalbard Archipelago in the north-western Barents Sea (Laberg and Vorren, 1996). Seismo-stratigraphic data indicate that the onset of glacially influenced sedimentation in the area occurred at about 1.8 Ma, when the Barents Sea Ice Sheet reached the continental shelf edge starting the build-up of the TMF systems (Knies *et al.*, 2009). These sediments are composed of amalgamated alternations of glacigenic debris flows and interglacial sediments (Laberg and Vorren, 1996; Pedrosa *et al.*, 2011). Multi-beam bathymetry and seismic reflection data on the Storfjorden TMF indicate the presence of three depositional lobes, referred to as Lobes I, II, and III from north to south (Pedrosa *et al.*, 2011) (Fig. 1A). The stratigraphic architecture of the three lobes changes from south to north with thicker and laterally continuous glacigenic debris flow in Lobe I and II with respect to Lobe III, and thicker post-glacial deposits on Lobe III with respect to the northern Lobes I and II (Pedrosa *et al.*, 2011).

Two main oceanographic currents affect the Storfjorden area (Fig. 1B): the shallow, warm, moderately saline West Spitsbergen Current (WSC), flowing northwards along the continental slope, and the cold, deeper, low-salinity East Spitsbergen Current (ESC) flowing as a coastal current. The former derives from the North Atlantic Current/Norwegian Atlantic Current (NwAC) (Johannessen, 1986), whereas the latter is a modified WSC that mixes with the polar waters and splits into the northern Spitsbergen margin, in the Arctic Ocean, to flow back to the Storfjorden Trough along the eastern and southern margins of the Spitsbergen archipelago. A branch of the ESC enters the Storfjorden Trough where it meets the WSC (Loeng, 1991). The thermal and saline gradients between these two water masses cause the development of the Polar Front (PF) to the north and the Arctic Front (AF) to the south, both variably located on the continental shelf of the Storfjorden Trough (Saloranta and Svendsen,

2001). The reconstruction of these water front shifts over time is very important as it influences the position of seasonal sea-ice coverage and, therefore, the primary productivity in the area (Stabell, 1986; Wollenburg *et al.*, 2004; Zamelczyk *et al.*, 2012).

Materials and methods

Three gravity cores (EG-01, EG-02 and EG-03) were collected on the Storfjorden TMF, during the EGLACOM cruise on board the R/V *OGS-Explora* (July–August 2008) (Fig. 1A; Table 1). Core EG-03 recovered the sediment–water interface that was, instead, lost in cores EG-01 and EG-02. One-centimetre-thick samples were collected at an average spacing of 10 cm (Fig. 2A–C). Planktonic and benthic and foraminifera were analysed in 83 samples, calcareous nannofossils in 92 samples and diatoms in 60 samples (Supporting Information, Tables S1–S4).

The samples were dried at 50 °C, weighed and wet-sieved using a stack of 63 μm. About 250 planktonic foraminifera were counted in the fraction >150 μm to compare the results with previous studies (CLIMAP) and the fraction 63–150 μm was qualitatively analysed. Planktonic foraminifera were counted and identified at the species level using the taxonomy of Hemleben *et al.* (1989) and Darling *et al.* (2006) for identification of the genus *Neogloboquadrina*. The density of planktonic foraminifera was reported as the number of individuals per gram of dry sediment (ind g^{-1}) (Fig. 2A–C). For the purposes of this study, we focused on the pattern of the three most abundant species (*Neogloboquadrina pachyderma*, *Neogloboquadrina incompta* and *Turborotalita quinqueloba*).

The whole fraction >63 μm was investigated for benthic foraminifera. Quantitative analyses were obtained counting about 300 tests when possible, and in foraminifera-rich sediments the samples were subdivided by dry splitting to obtain a sub-sample aliquot. Specimen counting was performed on well-preserved tests and recorded as relative abundance (percentage). Test fragmentation index was calculated as the rate of broken benthic foraminiferal tests with respect to the overall number of benthic foraminiferal tests. The benthic total abundance was reported as the number of individuals per gram of dry sediment (ind g^{-1}). The taxonomy of benthic foraminifera mainly followed the Arctic systematic studies of Feyling-Hanssen *et al.* (1971), Lagoe (1979), Scott and Vilks (1991), Ishman and Foley (1996) and Wollenburg and Mackensen (1998). The Ellis and Messina online catalogue of foraminifera (www.micropress.org/) was used for taxa description. Unilocular forms (*Fissurina*, *Lagena* and *Oolina*) and small Discorbidae were identified at a generic level only. Selected specimens were photographed using a scanning electron microscope (Leica Stereoscan 430i) at the University of Trieste, Italy (Fig. S1).

Sample preparation for calcareous nannofossil analyses followed the methodology described by de Kaenel and Villa (1996). Counting of specimens was performed on a fixed area of the slide equivalent to 1.57 mm^2, using a polarized-light microscope at a magnification of 1250×. Abundances were reported as number of coccoliths per 1.57 mm^2 in the slides.

Preparation of permanent mounts for diatom studies were accomplished according to the standard randomly distributed microfossils method. Absolute diatom numbers (no. of valves per gram of dry sediment) were determined using a Leica DMLB microscope at 1000× magnification. A count of at least 100 valves of non-dominant taxa per sample was performed using the method described by Schrader and Gersonde (1978). Over 300 valves per sample were generally measured. Sediment samples were considered barren if no valves were found along at least five transects. Species identification follows that of Tomas (1997).

Results

Age model

The age model used for this study follows Sagnotti *et al.* (2011) and Lucchi *et al.* (2013). The model was based on rock palaeomagnetic parameters and radiocarbon dates calibrated using Calib 6.0 software (Stuiver and Reimer, 1993), and applying an average marine regional reservoir effect $\Delta R = 84 \pm 23$ years (Mangerud and Gulliksen, 1975). The mean values of the calibrated age range $\pm 1\sigma$ were normalized to the calendar year (Table S5). Slight differences between the measured radiocarbon ages and the reconstructed age model are related to possible underestimation of the local regional reservoir correction applied during the calibration of mixed benthic and planktonic foraminifera. Indeed, Sarnthein (2011), Rae *et al.* (2014) and Thornalley *et al.* (2015) indicated that deep ocean waters after the LGM and during deglaciation were up to 1–2 ka BP older than they are today resulting in a higher local reservoir age. All the ages reported in the text as 'ka BP' represent calibrated ages before present (1950).

Sedimentary sequence

The stratigraphic sequence was subdivided into units following the acoustic and depositional units described by Pedrosa *et al.* (2011) and Lucchi *et al.* (2013), and the palaeoenvironmental reconstruction proposed by Lucchi *et al.* (2013). Core EG-01, collected from a minor gully located in the upper slope off Lobe I (water depth 1069 m below sea level, bsl), contains a major stratigraphic discontinuity between the older deposits of the core dating interglacial Marine Isotope Stage (MIS) 3 (>32 ka BP) and the ice-rafted debris (IRD)-rich sediments of the upper part dating to *ca.* 14 ka BP to the present (Fig. S2). This core contains only part of the deglaciation phase and it is considered only marginally important for the palaeoenvironmental reconstruction of this study. For these reasons, further lithological and paleontological results of core EG-01 will be reported in the Supplementary section and not discussed in detail here (Appendix S1 and Fig. S2). Core EG-02, located on the southern middle slope offshore Lobe III (water depth 1722 m bsl), contains a sequence spanning the last 16 ka BP. The deeper part of the sequence is formed by silty clay with abundant IRD related to ice-sheet collapse and by extensive subglacial meltwater input (interlaminated sediments), which occurred during the transition

Table 1. Core locations, water depth and total sediment recovery for the three cores from the Storfjorden Trough Mouth Fan.

Core ID	Lat N	Lon E	Water depth (m)	Location	Total recovery (cm)
EG-01	76°06.201′	13°37.625′	1069	Gully upper slope lobe II	220
EG-02	75°12.907′	13°04.587′	1722	Middle-slope lobe III	305
EG-03	75°50.615′	12°58.353′	1432	Middle-slope lobe II	291

from fully glacial to interglacial conditions (deglaciation) (Unit A2, Fig. 2A). The Holocene sedimentary sequence is composed of fine-grained, crudely layered and heavily bioturbated sediments that were deposited under the transport of persistent bottom currents (contourites) (Unit A1, Fig. 2A). Core EG-03, located on the middle slope off Lobe II (water depth 1432 m bsl), contains the last 12 ka BP depositional record. This core is characterized by an expanded Holocene sequence (acoustical Unit A1) (Fig. 2B).

Planktonic foraminifera

Planktonic foraminiferal assemblages are constituted by 11 species with a high dominance of *N. pachyderma*. Other species such as *T. quinqueloba* and *N. incompta* occurred with high percentages in the upper part of the sequences, whereas *Globigerina bulloides* and *Globigerinita glutinata* were present only in a few levels and at low percentages (Table S1). According to Darling *et al.* (2006) and Husum and Hald (2012), if the percentage of right coiling *N. pachyderma* is <3%, the specimens should be considered an aberrant form of left-coiling *N. pachyderma*. By contrast, when the percentage of the right-coiling *N. pachyderma* is higher than 3%, we considered these specimens as *N. incompta*.

Core EG-02 was divided into two different zones based on the overall planktonic foraminiferal abundance and assemblages (Fig. 3). In the lower part (300–150 cm, 16.2–12.1 ka BP), the biogenic fraction was scarce and/or absent (maximum

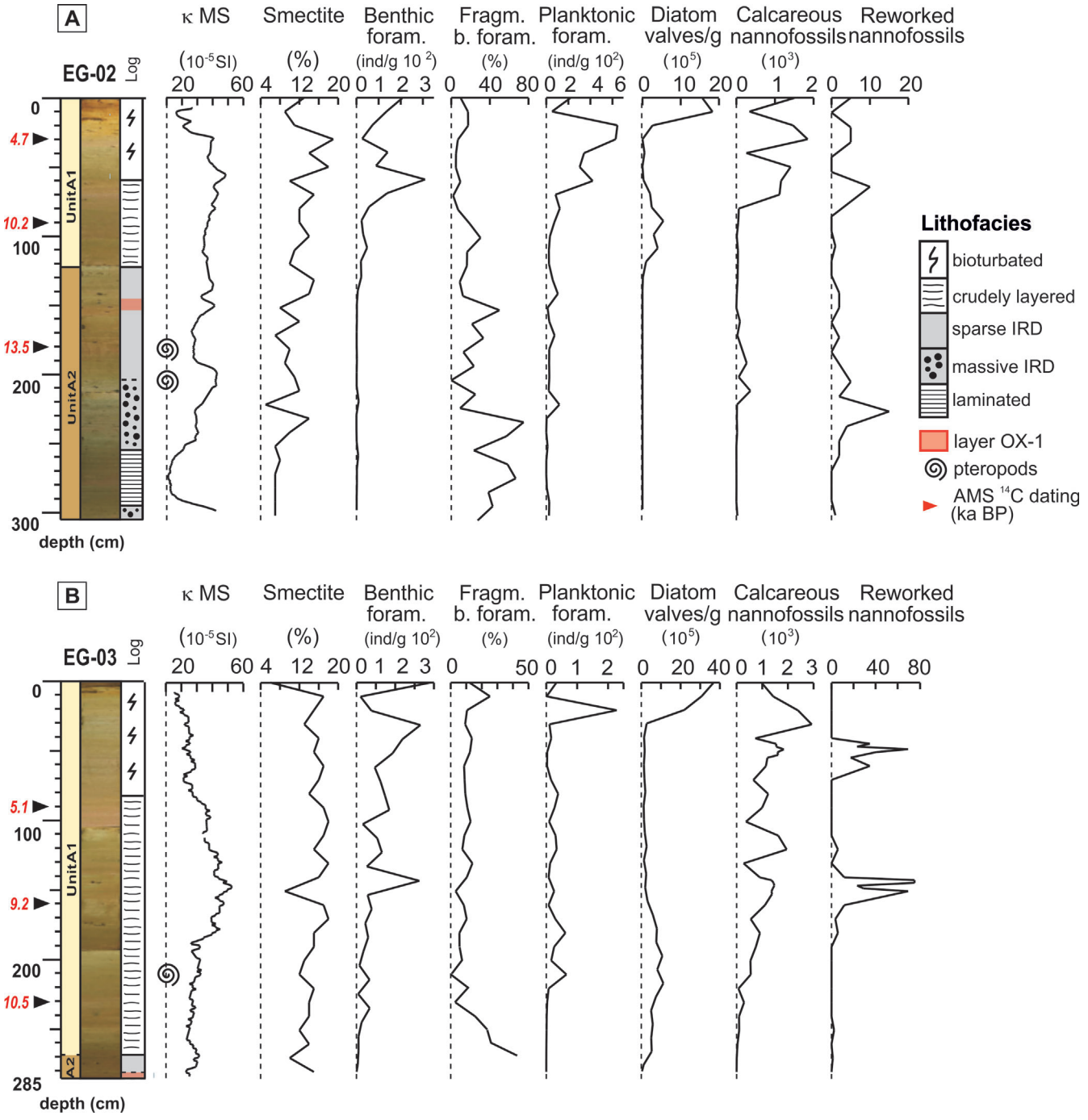

Figure 2. Lithological logs and down-core compositional characteristics of the two studied cores. Units A1 and A2 refer to the seismic facies (Pedrosa *et al.*, 2011; Lucchi *et al.*, 2013). Magnetic susceptibility after Sagnotti *et al.* (2011) and smectite data after Lucchi *et al.* (2013) are reported. Calcareous nannofossil abundance is expressed as the number of coccoliths 10 mm^{-2} in the slide. Calibrated ages before present (1950) – ka BP – are indicated in red.

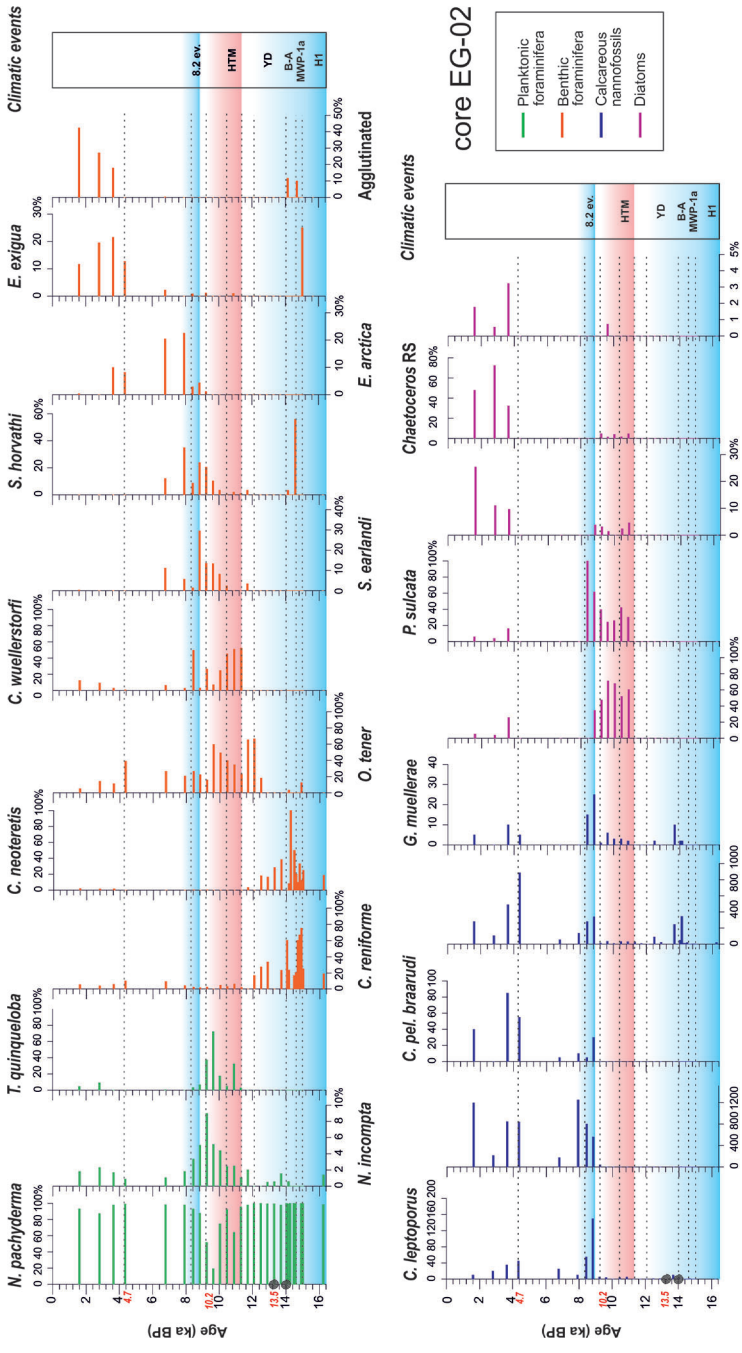

Figure 3. Down-core micropaleontological composition of core EG-02 plotted versus age. Dotted lines indicate the main events discussed in the text. Blue areas represent colder periods and red areas represent warmer periods. WSG = warm species group. The spiral on the left identifies pteropod presence. Calibrated ages before present (1950) – ka BP – are indicated in red. The top level of this core dates to 1.6 ka BP.

120 ind g^{-1}) with poor preservation and a presence of reworked Cretaceous calcispheres (Fig. 2A, S1). The planktonic foraminiferal assemblage, when present, was dominated by *N. pachyderma* with subordinate *N. incompta*. Well-preserved pteropod tests were recorded at 14.0 and 13.3 ka BP (Fig. S1). In the upper part of the core (12.1–1.6 ka BP), where abundance reached about 650 ind g^{-1}, *N. pachyderma* still dominated the assemblage although it decreased between 10.5 to 9.2 ka BP. *T. quinqueloba* reached percentages of about 50–70% and *N. incompta* attained its maximum relative abundance.

In core EG-03, the abundance of planktonic foraminifera was low, varying between 0 and 620 ind g^{-1}; only at level 20 cm did it reach values of about 2300 ind g^{-1}. *N. pachyderma* was the dominant species except between 9.7 and 8.7 ka BP where *T. quinqueloba* dominated (Fig. 4). In the upper part of EG-03 (7.7–0.05 ka BP), *T. quinqueloba* decreased strongly. *N. incompta* occurred with generally low percentages along the entire core. Peaks over 7% were recorded between 8.7–7.7 and 1.7–0.05 ka BP. Well-preserved pteropod tests were recorded at 9.9 ka BP.

Benthic foraminifera

The total abundance and species richness of benthic foraminifera were variable along the cores, with an increasing content and diversity in the uppermost sediments including several agglutinated taxa (Table S2).

In core EG-02, the total abundance reached the maximum of 310 ind g^{-1} at 60 cm. Very low values were recorded in the interlaminated facies and in the IRD-rich lithofacies where they were also poorly preserved (Fig. 2A). *C. reniforme* and *C. neoteretis* were the most common species at the base of the core (16.2–12.1 ka BP) (Fig. 3). Starting from *ca.* 12.1 ka BP, the assemblage is mainly characterized by *Oridorsalis tener, Cibicidoides wuellerstorfi, Seabrookia earlandi, Stetsonia horvathi, Epistominella arctica*. *E. exigua* became abundant only in the last 5 ka BP. The first occurrence of *C. wuellerstorfi* was recorded at 11.3 ka BP (Fig. 3).

In core EG-03, the total abundance gradually increased from the bottom to the top, where it reached the maximum of 382 ind g^{-1} (Fig. 2B). The benthic foraminifera were poorly preserved at the base of the core (fragmentation until 41% at 270 cm). Benthic foraminifera were absent at the bottom, whereas the crudely laminated facies were characterized by *C. reniforme, O. tener, C. wuellerstorfi, M. barleeanus, S. earlandi* and *S. horvathi* (Fig. 4). The last 5 ka BP were mainly characterized by *C. neoteretis, E. arctica* and *E. exigua*.

Calcareous nannofossils

The lower part of core EG-02 (16.2–14.2 ka BP) did not contain nannofossils, while reworked Palaeogene and Cretaceous taxa were recovered at around 14.4 ka BP within the IRD-rich lithofacies. The highest nannofossil abundance was recorded from 9.2 ka BP upward, although the sequence contained two minima recorded at 40 and 10 cm (Fig. 2A). The assemblage was characterized by *Calcidiscus leptoporus, Coccolithus pelagicus* s.l. (*C. pel. pelagicus* and *C. pel. braarudi*), *Emiliania huxleyi* and *Gephyrocapsa muellerae* which peaks at about 8.2 ka BP (Fig. 3; Table S3). These species can provide information on sea surface temperature; *Calcidiscus leptoporus* is reported as having different lower temperature limits (up to 11 °C) (Samtleben *et al.*, 1995), *C. pelagicus* and *G. muellerae* are known to prefer cool waters, while *E. huxleyi* is a euryhaline and eurythermal coccolith (Roth and Coulbourn, 1982).

The older part of core EG-03 (below 250 cm) did not contain nannofossils, whereas reworked taxa were observed at 150 and 50 cm (Fig. 2B). The highest nannofossil abundance was recorded in the upper sediments from about 8.5 ka BP, with an association dominated by *E. huxleyi* and *C. pel. pelagicus*. The assemblage also contains *G. muellerae, C. leptoporus* and *C. pel. braarudi* (Fig. 4). The distribution of *G. muellerae* showed two main peaks located at about 8.2 and 2–3 ka BP (Fig. 4). An abrupt decrease in nannofossil abundance was recorded at 130 cm (7.2 ka BP) (Fig. 2B).

Diatoms

Diatoms are generally absent in the IRD-rich lithofacies of cores EG-02 and EG-03 (Fig. 2A,B; Table S4). In core EG-02, diatoms appeared at about 11.3 ka BP (131.5 cm, Fig. 2A). Their overall abundance was characterized by two distinct maxima centred approximately in the middle part of the crudely layered interval at 10.5 and 9.6 ka BP (110 and 90 cm, respectively) and in the uppermost part of the heavily bioturbated sediments, with an abundance of 1.8×10^6 valves g^{-1} at 2.8 ka BP (10 cm deep, Fig. 2A). An abrupt decrease in abundance from 2.4 to 1.3 ka BP (50–30 cm) was in evidence, with values two orders of magnitude below the maximum (Fig. 2A). The former peak was mainly characterized by *Coscinodiscus* spp. (up to 90%) associated with *Paralia sulcata* and subordinately with *Thalassiosira* spp. and *Chaetoceros* RS (resting spores) (Fig. 3). The latter peak was characterized by a decreasing abundance of *Coscinodiscus* spp. and *P. sulcata*, and a relative increase in *Chaetoceros* RS (up to 70% of the assemblage) with *Thalassiosira* spp. and a group of species considered here to be a Warm Species Group (WSG), that included *Azpeitia* spp., *Hemidiscus cuneformis, Rhizololenia bergonii, Roperia tessellata, Thalassiosira oestrupii* (Koç-Karpuz and Schrader, 1990; Tomas, 1997).

In core EG-03, diatoms appeared at 11.3 ka BP (270 cm), corresponding to the base of the crudely layered interval (Fig. 2B). Similar to the previous core, their overall abundance was characterized by three maxima centred approximately in the middle part of the crudely layered interval at 10.0 ka BP (220 cm) and 9.5 ka BP (200 cm), and in the uppermost part of the heavily bioturbated sediments, with an abundance of 3.6×10^6 valves g^{-1} at the top of the core. *Coscinodiscus* spp. and *Rhizosolenia* spp. associated with *P. sulcata* define the assemblage at the base of this core. At the same time, the group of WSG species reached its highest abundance in this interval. *Paralia sulcata* was very abundant in the interval 7.7–3.3 ka BP (Fig. 4). The uppermost peak was characterized by a decreasing abundance of *Coscinodiscus* spp. and *P. sulcata* and a relative increase in *Chaetoceros* RS (up to 80% of the assemblage) with *Rhizosolenia* spp. and *Thalassiosira* spp. (Fig. 4).

Discussion

In the following we will discuss the last deglaciation (16.2–11.7 ka BP) and the Holocene subdivided into: Early Holocene and Holocene Thermal Maximum (HTM) event, the 8.2 ka cold event, the 8.2–4 ka and 4.0 ka to Recent time intervals, recorded in cores EG-02 and EG-03.

The last deglaciation: 16.2–11.7 ka BP

The last deglaciation phase is represented by Unit A2 in cores EG-02 and EG-03 (Fig. 2A–C). Core EG-02 recorded an expanded deglacial sequence, whereas core EG-03 contains

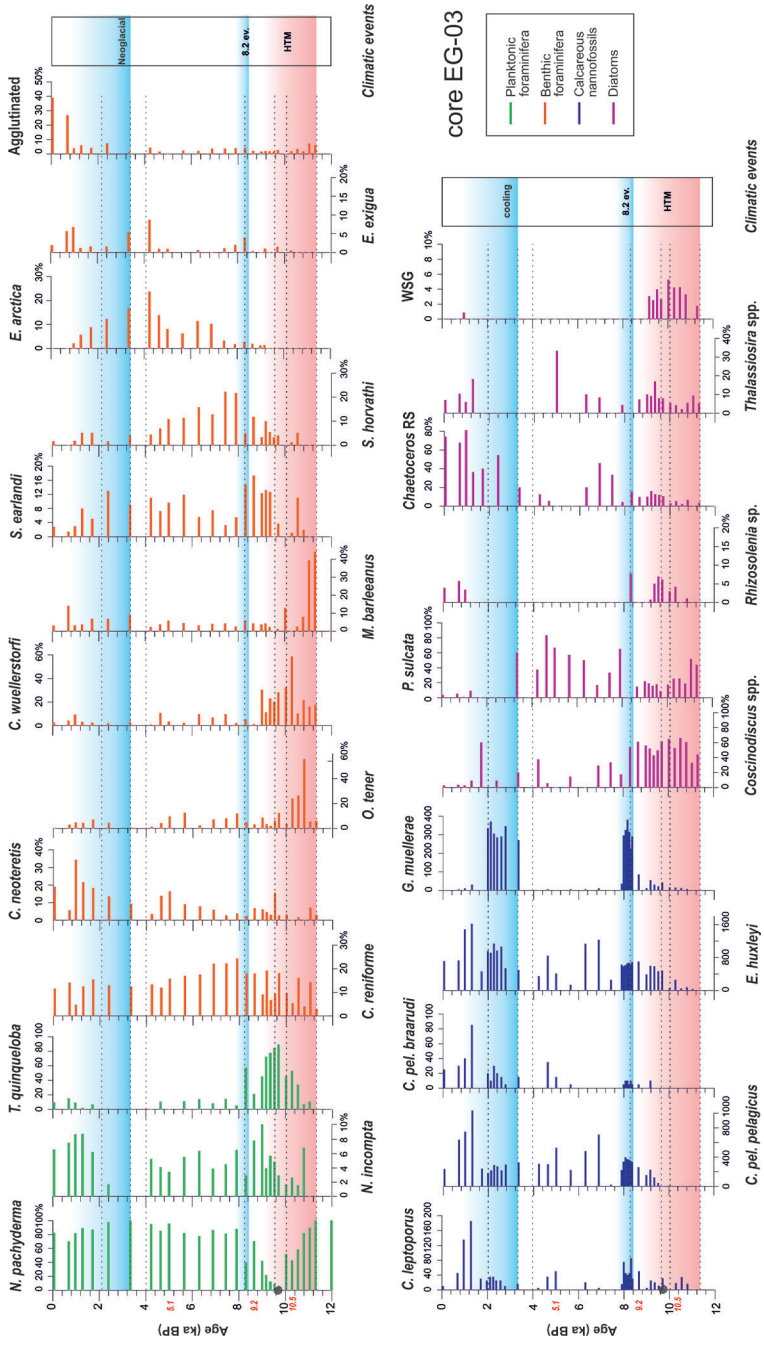

Figure 4. Down-core micropaleontological composition of core EG-03 plotted versus age. Dotted lines indicate the main events discussed in the text. Blue areas represent colder periods and red areas represent warmer periods. WSG = warm species group. The spiral on the left identifies pteropod presence. Calibrated ages before present (1950) – ka BP – are indicated in red.

only the later stage of deglaciation recorded in the bottom of the core (Lucchi *et al.*, 2013).

The deglaciation is characterized in core EG-02 (305–295 cm, Fig. 2A) by coarse–massive IRD-rich sediments and by a peak of magnetic susceptibility similar to that recognized in sediment cores from the same area (Rasmussen *et al.*, 2007; Jessen *et al.*, 2010). Lucchi *et al.* (2013) correlated this magnetic peak to Heinrich event H1, dated to 16.8 ka BP. Benthic calcareous foraminifera are extremely poor and represented by *Cassidulina* spp., whereas the low-density monospecific (*N. pachyderma*) planktonic foraminiferal assemblage indicated that the surface water over the slope was influenced by polar water (Fig. 5). There is no evidence of the 'benthic Atlantic species' described for this period in core JM03-373 by Rasmussen *et al.* (2007).

The interlaminated sediments above the IRD-massive deposits were interpreted as plumites derived from meltwater discharge from the Storfjorden–Kveithola glacial system and associated with the meltwater pulse (MWP)-1a (Lucchi *et al.*, 2013, 2015). This event is recorded all along the western Svalbard continental margin and Kveithola TMF (e.g. Jessen *et al.*, 2010; Jessen and Rasmussen, 2015; Carbonara *et al.*, 2016), and can be used as a time marker horizon dated to approximately 14.7–14.3 ka BP (Deschamps *et al.*, 2012), and it corresponds to the early Bølling Interstadial (Kienast *et al.*, 2003) (Fig. 5). In this level the very scarce abundance of planktonic foraminifera (dominated by *N. pachyderma*), and nannoplankton, and the absence of diatoms indicate deteriorated surface water conditions, probably having been affected by a more extensive sea-ice cover in winter and meltwater layer during spring. Even if statistically non-representative, the presence of *C. reniforme* and *C. neoteretis* during this interval may indicate the influence of cold and salty AW at the bottom of the middle slope, in agreement with Rasmussen *et al.* (2007) (Table 2). The preservation of the foraminiferal tests is very poor (fragmentation up to 60%, Fig. 2A) suggesting both mechanical damage and water corrosion.

The overlying massive IRD-rich sediments (Fig. 2A, core EG-02: 14.3–14.0 ka BP) indicate the progressively stronger influence of AW over the area, shown by the occurrence of rare *E. huxleyi*, among the planktonic taxa (Fig. 3). The increasing influence of AW is also indicated by the gradual increase in the percentages of smectite in the clay mineral assemblage (Fig. 2A,B) (Lucchi *et al.*, 2013), as suggested by Junttila *et al.* (2010), and hence supporting the correlation with the Bølling–Allerød warm phase (Fig. 5). The presence of reworked Palaeogene and Cretaceous nannofossil taxa, together with Cretaceous calcispheres in the massive IRD-rich sediments (EG-02, 250–210 cm, Fig. 2A), confirms sediment release by the ice front during the final phase of the deglaciation. The abundant occurrence of pteropods (*Limacina helicina*, Fig. S1) in core EG-02 at *ca.* 14.0 and 13.3 ka BP (Fig. 5) confirms the favourable environmental conditions with massive input of sediments that allowed the rapid burial of the pteropod specimens after deposition, resulting in the

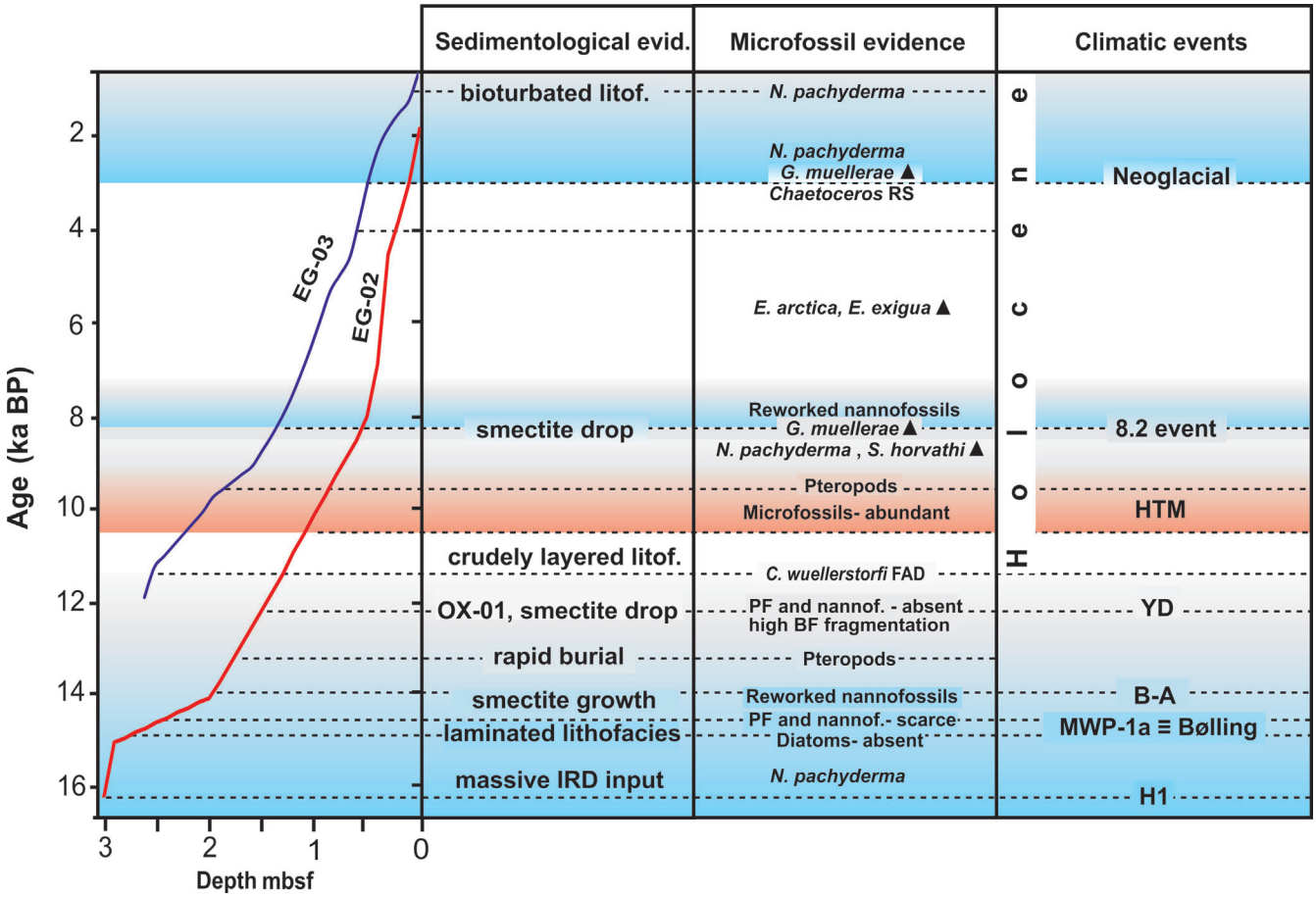

Figure 5. Age–depth plot for the two investigated cores. The main climatic and palaeoenvironmental events are illustrated, supported by sedimentological and micropalaeontological evidence. The blue areas represent colder periods and the red area represents a warmer period. Horizontal dotted lines limited the recognized events with related ages on the left axis. H1 = Heinrich event 1, MWP-1A = Meltwater Pulse 1A, B-A = Bølling–Allerød, YD = Younger Dryas, OX-01 = oxidized level, HTM = Holocene Thermal Maximum. BF = benthic foraminifera; PF = planktonic foraminifera. Black triangles indicate increasing relative occurrence of the species.

Table 2. Taxonomy and ecology of the most abundant planktonic and benthic foraminiferal species recorded in the three studied cores.

Foraminifera species	Ecological chatacters	References
Neogloboquadrina pachyderma	Polar species related to Arctic and Polar waters, living at or just below the depth of the maximum chlorophyll concentration, which it exploits as a food source zone. It ingests either phytoplankton or detrital chlorophyll.	Hemleben *et al.* (1989); Kohfeld *et al.* (1996)
Neogloboquadrina incompta	Sub-polar species associated to warm Atlantic water. It occupies the upper 60 m of the water column and its seasonal peak abundance is in late summer.	Hemleben *et al.* (1989); Schiebel *et al.* (2001); Schiebel and Hemleben (2000)
Turborotalita quinqueloba	Near surface dweller sub-polar species associated to Arctic waters and Arctic/Polar fronts	Hemleben *et al.* (1989)
Cibicidoides wuellerstorfi	Near surface dweller sub-polar species associated to Arctic waters and Arctic/Polar fronts	Lutze and Thiel (1989); Wollenburg and Mackensen (1998)
Cassidulina neoteretis	Infaunal species confined to areas influenced by cool, slightly transformed subsurface Atlantic Water (AW) with stable salinity	Ishman and Foley (1996); Jennings *et al.* (2004); Lagoe, 1979; Lubinski *et al.* (2001); Osterman *et al.* (1999); Wollenburg *et al.* (2004)
Cassidulina reniforme	Arctic-Polar species linked to cold and salty AW, and locally related to distal glaciomarine environments especially if associated to E. excavatum. Occasionally indicates establishment of dysoxic or periodic anoxic conditions at the bottom	Hald and Korsun (1997); Korsun and Hald (2000); Polyak *et al.* (2002); Steinsund, 1994
Cibicides lobatulus	Epifaunal species correlated with coarse sediments and high hydrodynamism	Hald and Korsun (1997); Murray, 2006; Schröder-Adams *et al.* (1990)
Epistominella arctica	Arctic areas with low to no bottom current activity and characterized by seasonally ice-free areas; affinity with both low-productivity evnvironments and phytoplancton blooms	Gooday, 1993; Wollenburg and Mackensen (1998); Wollenburg and Kuhnt (2000)
Episominella exigua	Opportunistic species able to feeding on fresh phytodetritus	Gooday, 1993; Thomas *et al.* (1995); Wollenburg and Mackensen (1998)
Ioanella tumidula	Seasonally ice-free areas between 1500–3000 m; opportunistic phytodetritus feeders, unpredictable food productivity	Thomas *et al.* (1995); Wollenburg and Mackensen (1998)
Islandiella helenae / I. norcrossi	"Low arctic conditions" characterised by high seasonal productivity; also in distal glacio-marine sediments	Korsun *et al.* (1995); Korsun and Hald, 1998; Pogodina, 1999; Stenisund, 1994
Melonis barleeanus	Arctic–Boreal infaunal species related to Atlantic-derived water with supply of degraded organic matter; high salinities	Caralp, 1989; Jennings *et al.* (2004); Polyak *et al.* (2002)
Oridorsalis tenerus	Low productivity area in water depth of 2000–3000 m	Osterman *et al.* (1999); Wollenburg and Mackensen (1998)
Seabrookia earlandi	Rarely recovered, it represents oxic surface sediments and in presence of symbiotic methane-and sulfur-oxidizing bacteria	Wollenburg and Mackensen (2009)
Stetsonia horvathi	Presently restricted to permanently ice-covered areas at water depth >2200 m, or in areas with seasonal sea ice with low or instable phytodetritus accumulation values	Husum *et al.* (2015); Lagoe, 1977; Wollenburg and Mackensen (1998)

preservation of the aragonite tests. The presence of pteropods during the same interval in Arctic sediment has also been reported by Ślubowska-Woldengen *et al.* (2007) and Consolaro *et al.* (2018).

The benthic foraminifer fragmentation increases considerably in the interval between where the oxidized layer (OX-1) was identified (Fig. 2A), suggesting the dissolution of calcium carbonate probably related to this period. This layer has been interpreted by Lucchi *et al.* (2013) as the expression of the Younger Dryas (YD) cold event or its termination (Broecker *et al.*, 2010). The absence of nannofossils and *N. incompta* in the oxidized layer supports the cold conditions of the superficial water column also suggested by a drop of smectite concentration (Lucchi *et al.*, 2013), which is linked to AW transportation and, consequently, to its influence (Junttila *et al.*, 2010) (Fig. 5). Cool conditions for this period from the north-western Barents Sea margin have also been reported by Rasmussen *et al.* (2007) and Consolaro *et al.* (2018).

Early Holocene and HTM event

The upper acoustic Unit A1 records the onset of the Holocene (Fig. 2A,B). The low percentage of fragmentation of benthic foraminifera indicates a reduced influence of the sedimentary glacial processes. Just above the boundary between Units A2 and A1, at about 11.3 ka BP, the first appearance of the epibenthic suspension-feeder foraminifer *C. wuellerstorfi* confirms the influence of strong bottom currents evidenced for this Unit (Lucchi *et al.*, 2013) (Figs 3 and 4; Table 2). The sudden occurrence of *C. wuellerstorfi* follows the end of the YD (Fig. 5) which can be considered nearly synchronous in the Storfjorden area as well as the south-western margin of Svalbard (Sarnthein *et al.*, 2003). This bioevent was recorded by Rasmussen *et al.* (2007) in the Storfjorden TMF slope at about 10 ka ^{14}C BP (accelerator mass spectrometry dating corrected by reservoir effect only) and in the eastern Fram Strait at about 11.0 ka BP by Consolaro *et al.* (2018) and is considered the first warming indication of bottom water after the YD. In addition, the benthic assemblage includes *C. reniforme*, *O. tener* and *M. barleeanus* (mainly in core EG-03) (Figs 3 and 4). The significant occurrence of both *C. wuellerstorfi* and *O. tener* indicates conditions similar to the modern deep-sea slopes of the Nordic Seas (Sejrup *et al.*, 1981; Mackensen *et al.*, 1985); *M. barleeanus* suggests the influence of relatively warm AW with a supply of degraded organic matter (Table 2). It is noteworthy that in the same time interval the presence of *C. neoteretis* is mostly <10% in core EG-03, and it is almost absent in core EG-02 (Figs 3 and 4), in agreement with Rasmussen *et al.* (2007) and Consolaro *et al.* (2018). *C. neoteretis* is common in the Arctic Ocean and it indicates subsurface AW masses and not permanently

ice-covered conditions (Table 2), but the relationship with this water is still subject to debate (Osterman *et al.*, 1999; Wollenburg *et al.*, 2004). Knudsen *et al.* (2008) suggest its possible relation with some specific nutrient content of the AW. Its reduced presence could suggest a reduced influence of subsurface AW masses during the onset of the Holocene but it could also indicate that the AW was strongly mixed with shelf waters, as suggested by Lubinski *et al.* (2001) in the Kara and Barents Seas. The possible influence of shelf waters could be supported by the contemporary presence of the diatom *Paralia sulcata*, a neritic species characteristic of coastal upwelling conditions (Abrantes, 1988) (Figs 3 and 4).

Starting from about 11.3 ka BP, a significant occurrence of diatoms dominated by *Coscinodiscus* spp., together with *P. sulcata*, *Thalassiosira* spp., *Rhizosolenia* spp., WSG species (especially for core EG-03), and subordinate *Chaetoceros* RS is recorded in cores EG-02 and EG-03 (Figs 3 and 4). The high abundance of *Coscinodiscus* spp. with a relatively high abundance of WSG species is related to warm AW masses and was suggested as a chronostratigraphic marker for the early Holocene in the western Svalbard slope area (Jessen *et al.*, 2010). Furthermore, the coexistence of this genus together with *Rhizosolenia* spp. (Fig. 4) could also indicate a deepening of the nutricline (Kemp *et al.*, 2000; Kemp and Villareal, 2013). *P. sulcata* is a bottom species very common in the Nordic Seas associated with the Norwegian-Atlantic current (Koç-Karpuz and Schrader, 1990; McQuoid and Nordberg, 2003). The relatively high content of *P. sulcata* could indicate high primary productivity (Abrantes, 1988). Nevertheless, the abundant presence of *P. sulcata* should be related to silica preservation, as their frustules are highly silicified and reflect differential dissolution (Bárcena and Abrantes, 1998). The overall increased abundance of diatoms at 10.5–9.2 ka BP in this study corresponds to a period of higher sea surface temperatures and high primary productivity. The slightly different ages of the maximum diatom concentration observed between the two studied cores are probably due to sampling resolution (every 10 cm) rather than to a different age of these bioevents. These results are comparable with those found by Jessen *et al.* (2010), Carbonara *et al.* (2016) and Consolaro *et al.* (2018) in the Storfjorden TMF slope and in the eastern Fraim Strait, and according to Stabell (1986), the high diatom productivity signal can be used as an indicator of PF retreat.

A sea surface temperature optimum is also indicated by the low relative abundance of *N. pachyderma*, and an increase in productivity is indicated by *T. Quinqueloba*, which formed more than 60% of the planktonic fauna at around 9.8–9.2 ka BP (Figs 3 and 4). Our data correspond well with those of Rasmussen *et al.* (2007), Aagaard-Sørensen *et al.* (2014), Carbonara *et al.* (2016), Werner *et al.* (2016) and Consolaro *et al.* (2018), all recording similar variation in the planktonic assemblage in the same time interval. This period, known as the HTM (Kaufman *et al.*, 2004; Renssen *et al.*, 2009, 2012) (Fig. 5), has been evidenced in the Nordic Seas in several climate archives in a period approximately between 10 and 6 ka BP (Risebrobakken *et al.*, 2011). Sites from the shelf and upper slope of western and northern Svalbard generally show a noticeable but more limited influence of AW (Ślubowska *et al.*, 2005; Ślubowska-Woldengen *et al.*, 2007), probably due to the influence of colder and less saline surface waters, originating from the remaining ice caps over Svalbard. The elevated microfossil abundance in the early Holocene sediments suggests an extraordinarily vigorous water inflow from the south during the HTM, probably through the Fram Strait and across the Barents Sea. The HTM mainly reflects the strong early Holocene summer insolation, which influenced the superficial mixed layer temperatures of the Nordic Seas (Risebrobakken *et al.*, 2011 and references herein). The increase in shade flora in the studied cores, mainly represented by *Coscinodiscus* spp. and *P. sulcata* (Figs 3 and 4), probably indicates the deepening of the nutricline because of the increased input of fresh and turbid waters in the ocean due to meltwater from ice-sheets or inland glaciers.

Abundant pteropod tests of *L. helicina* were observed at 9.7 ka BP (Fig. 5) corresponding to a diatom concentration increase. We argue that the preservation of the aragonite test in the sediments may be related to the rapid burial of the pteropod tests by diatom mats.

Nannofossil species diversity at the beginning of the Holocene is low. The assemblage is dominated in this period by cold-water-adapted taxa such as *C. pelagicus* s.l. and *G. muellerae* (Roth and Coulbourn, 1982; Samtleben and Bickert, 1990; Samtleben *et al.*, 1995; Wells and Okada, 1997). During the HTM, the nannofossil assemblage, mainly represented by *C. leptoporus* and *E. huxleyi*, registered a weak increase (Fig. 2A,B), suggesting seasonal ice-free conditions and warming of the surface waters, as also indicated by the alkenone data in the Nordic Seas by Risebrobakken *et al.* (2011) for the same climatic event.

The 8.2 ka cold event

A decreasing abundance in *C. wuellerstorfi* is recorded in cores EG-02 and EG-03, from about 10.0 to 7.9–7.4 ka BP (Figs 3 and 4) suggesting a weakening in the lateral currents, in agreement with Rasmussen *et al.* (2007). Starting from about 9.6 ka BP up to about 8.0 ka BP, a consistent increase in *S. horvathi*, *C. reniforme* and *S. earlandi* has been noted (Figs 3 and 4).

Stetsonia horvathi is a small polar species (<70 μm) that is adapted to live both under permanent or seasonal sea ice, associated with low and unstable organic flux to the seafloor (Table 2) at a water depth >2200 m in the Arctic Ocean. It has been used as a proxy for glacial conditions during the Pleistocene (Polyak *et al.*, 2013; Lazar and Polyak, 2016). The simultaneous presence of planktonic foraminifera and calcareous nannoplankton excludes the possibility of permanent sea ice conditions for this area (Villa *et al.*, 2012). The increase in *C. reniforme* suggests a renewal of the cold and salty AW, but might also indicate the establishment of dysoxic or periodic anoxic conditions at the bottom (Table 2). *S. earlandi* (Fig. S1), a small species rarely recorded in the north-western Barents Sea, was reported by Wollenburg and Mackensen (2009) as living in the hummocky peripheral part of the Håkon Mosby mud volcano located at a water depth of 1265 m on the south-western Barents Sea slope, under conditions of anoxic surface. The increase in these species could indicate a period of oligotrophic conditions at the sea bottom that was associated here with the 8.2 ka BP cold event.

The increase in the cold nannofossil species *G. muellerae*, at about 8.2 ka BP, suggests cooling conditions in the surface waters as well (Fig. 5). This species is presently related to subarctic cold water (Henderiks and Bollmann, 2004), although the milder ecological preference of *G. muellerae* has been reported (e.g. Flores *et al.*, 1997; Dylmer *et al.*, 2013). The peak of PF indicator species *T. quinqueloba* and the decrease of the temperate species *N. incompta* with the subsequent total dominance of *N. pachyderma* suggest a short-term change of the water masses, between 8.2 and 7.9 ka BP (Figs 3 and 4) (Rasmussen *et al.*, 2007; Knudsen *et al.*, 2008). In addition, the sharp decrease in smectite content in these levels could also suggest the reduced influence of AW (Fig. 5). All this evidence leads us to associate this interval with the cold event which occurred in

the Northern Hemisphere at about 8.2 ka BP (Rohling and Pälike, 2005; Ellison et al., 2006). This interpretation is also supported by the magnetic susceptibility curve of both cores EG-02 and EG-03 (Lucchi *et al.*, 2013), showing a characteristic peak during the Holocene at 55 and 147 cm, respectively (Fig. 2B,C), dated 8.2 ka BP in the Western Svalbard slope (Jessen *et al.*, 2010).

Time interval 8.2–4.0 ka BP

From 8.2 ka BP up to about 4.0 ka BP, a decrease in *S. horvathi* and *C. reniforme* is recorded in core EG-03 together with a relative increase in the benthic foraminifera *E. arctica*, *C. neoteretis* and *E. exigua* (Figs 3 and 4), in agreement with Consolaro *et al.* (2018). *E. arctica* occurs in seasonally ice-free Arctic areas with low to no bottom current activity and together with *E. exigua* may also feed on phytodetritus (Wollenburg and Mackensen, 1998; Cornelius and Gooday, 2004). *E. arctica* is considered to have a transitional ecological strategy from permanent to seasonal sea ice conditions (Wollenburg and Kuhnt, 2000). Its increasing abundance in this study seems to indicate a reduction in the oligotrophic conditions previously suggested by *S. horvathi*, possibly related to the variation of the year-round ice cover of the upper water column. Furthermore, the increasing occurrence of *C. neoteretis* and the relative decrease in *C. reniforme* suggest the increasing influence of the warmer subsurface bottom water. The decrease in *G. mullerae* together with a weak drop in *C. pelagicus* s.l. and a rise in *P. sulcata* (core EG-03 only) suggest warmer conditions for the upper water column as well. A sudden drop in the presence of *T. quinqueloba* could indicate a significant decrease in surface water productivity, together with relatively stable and milder temperature conditions (Rasmussen *et al.*, 2014). This would be in agreement with Sarnthein *et al.* (2003), who found evidence of extended phases of a general slight warming during the cool Late Holocene and, in particular, from 6.5 to 4.2 ka BP. By contrast, the high proportion of *T. quinqueloba* was seen by Consolaro *et al.* (2018) in the eastern Fram Strait for the period from 6.2 to 4.1 ka BP. Thus, the significant decrease in *T. quinqueloba* in our study could also be related to a preservation factor. This species is in fact considered a dissolution-prone species (Zamelczyk *et al.*, 2012) if compared to other planktonic species.

Time interval 4.0 ka BP to Recent

The upper sequence of EG-03, from about 3.2 ka BP (the last 60 cm), is characterized by a further increase in *C. neoteretis* and by a decrease in *E. arctica* (Fig. 4). At the same time, *E. exigua* increases in agreement with an increase in diatom concentration described below (Figs 3 and 4), indicating a strong seasonal pulse of fresh phytodetritus for this period (Table 2). In this interval, the high abundance of agglutinated foraminifera occurs (Fig. S1). Their abundance (recorded only in the more recent sediments) could indicate a weak diagenetic process that generally tends to disintegrate the tests towards the bottom of the core. From 3.2 to 2 ka BP *G. muellerae* shows a general increase, whereas *T. quinqueloba* and *P. sulcata* nearly disappear, suggesting a new cooling trend in the studied area (Fig. 5). The reduction of *T. quinqueloba* in this period could be related to a decreasing advection of the warmer AW rather than to AF fluctuation, in agreement with Werner *et al.* (2016). This period should correspond to the so-called Cool Late Holocene (Andersen *et al.*, 2004), known also as the Neoglacial cold event. Further evidence, however, is needed to support this interpretation.

A small amelioration of the surface water condition is apparent for the last 2 ka BP, testified to by the increase in the temperate species *N. incompta*, as also suggested by Rasmussen *et al.* (2014). In this period a sharp increase in diatoms indicates increasing seasonal productivity (Fig. 2A, B). Although there is a significant difference in the age of the diatom peaks in the two cores, the association is characterized mainly by *Chaetoceros* RS and subordinately by *T. nitszchioides*, *Thalassiosira* spp. and *Rhizosolenia* spp. (Figs 3 and 4; Table S4). *Chaetoceros* is one of the most abundant diatom genera in modern oceans; it is present in most environments from coastal temperate to Polar Regions. *Chaetoceros* RS have traditionally been interpreted as indicative of very high primary productivity (Williams, 1986; Koç-Karpuz and Schrader, 1990; De Sève, 1999). Phytoplankton blooms large enough to deplete nutrients are rare in polar areas and depend on the increased stratification of the upper water column and the presence of a shallow mixed layer (Leventer *et al.*, 1996). In Polar Regions, the abundance of over 20% in *Chaetoceros* RS could be related to sea ice duration >3 months a^{-1}, with an optimum coverage of 3–9 months a^{-1} (Armand *et al.*, 2005). Leventer *et al.* (1996) suggested that this high abundance could be related to surface water stratification produced by sea ice meltwater, in agreement with the presence of *Rhizosolenia* spp., which has been considered a shadow species adapted to live in the lower photic zones under conditions of stratification (Kemp *et al.*, 2000). Moreover, *Thalassionema nitzschioides* (not shown) has been reported as a cosmopolitan species. Bárcena and Abrantes (1998) considered that these species could be associated with occasional upwelling and/or freshwater discharge; this assumption could be in agreement with seasonal sea-ice melting. Cooling conditions of the surface water masses at about 0.6 ka BP were identified by a decrease in the nannofossil total abundance together with a slight decrease in the warm-water taxa such as *N. incompta* and *Coscinodiscus* spp.

Conclusions

The integrated micropalaeontological (planktonic and benthic foraminifera, calcareous nannoplankton and diatoms) investigations of two sediment cores (EG-02 and EG-03) recovered from the middle/upper slope of the Storfjorden TMF add new data to the Late Quaternary reconstruction of the palaeoenvironmental and palaeoceanographic conditions of this region. Two intervals of significant palaeoenvironmental/climate change were identified: the last deglaciation (16.2–11.7 ka BP) and the Holocene.

The last deglaciation conditions were dominated by a massive input of terrigenous sediments (plumites of MWP-1A) which largely diluted the biogenic fraction in the sedimentary record, determining environmental conditions hostile to bio-productivity and test preservation. The early Holocene was characterized by a sharp recovery of productivity (mainly planktonic foraminifers and diatoms) and microfossils). On the bottom, the benthic foraminifer *C. wuellerstorfi* marks the occurrence of contour currents that characterized the beginning of the Holocene at 11.3 ka BP. The prominent flowering of diatoms heralded the HTM between 10.5 and 9.2 ka BP. An optimum of the surface water temperature together with an increase in productivity were indicated also by the planktonic fauna. The occurrence of small benthic foraminifera species such as *S. horvathi* and *S. earlandi* suggests progressive oligotrophic bottom conditions after the HTM, whereas the cooling

conditions of surface waters during 8.3–8.2 and at 2.4 ka BP were indicated by the increased presence of the cold-water nannofossil species *G. muellerae* and the planktonic foraminifer *N. pachyderma*. High primary productivity is again recorded by the sharp increase in *Chaetoceros* RS during the late Holocene at about 2.4–1.0 ka BP, suggesting seasonal sea-ice melting. Cooling conditions of the surface water masses at about 0.6 ka BP were identified by a decrease in the nannofossils together with a decrease in the warm-water taxa such as *N. incompta* and *Coscinodiscus* spp.

The integrated use of diverse microfossil proxies is important because they do not always respond to major palaeoclimate forces. Close similarities were recorded mainly between planktonic foraminifera and diatoms. Moreover, the benthic species >63.5 μm were very useful as a proxy of trophic bottom water conditions.

Acknowledgements. This study was supported by the Italian projects OGS-EGLACOM and PNRA-MELTSTORM, the Spanish SVAIS (POL2006-07390), NICESTREAMS, and DEGLABAR (CTM2010-17386) projects, the Danish GEUS project 'Foraminifera in Artic Ocean', and 'CORIBAR-DK', CARLSBERG project, no. 2012_01_0315. Special thanks to A. Camerlenghi for his continuous scientific support and encouragement. Many thanks to Karolyn Close for linguistic revision. The authors thank two anonymous reviewers for their constructive comments which greatly improved the quality of the manuscript.

Supplementary information

Appendix S1. Core EG-01 descriptions and results.

Figure S1. Scanning electron photomicrographs of some foraminifer species representative of the palaeoenvironments recorded in the EGLACOM cores (magnification: bar = 30 μm): 1 - *Astrononion gallowayi*, side view; 2 - *Cibicides lobatulus*, umbilical side view; 3 - *Cibicidoides wuellerstorfi*, umbilical side view; 4 - *Cassidulina reniforme*, side view; 5 - *Cassidulina neoteretis*, side view; 6 - *Epistominella exigua*, spiral side view; 7 - *E. exigua*, umbilical side view; 8 - *Epistominella arctica*, spiral side view; 9 - *E. arctica*, umbilical side view; 10 - *Eilohedra nipponica*, spiral side view; 11 - *E. nipponica*, umbilical side view; 12 - *Stetsonia horvathi*, umbilical side view; 13 - *S. horvathi*, spiral side view; 14 - *Stainforthia fusiformis*, side view; 15 - *Stainforthia loeblichi*, side view; 16 - *Melonis barleeanus*, side view; 17- *Oridorsalis tener*, spiral side view; 18 - *Seabrookia earlandi*, side view; 19 - *S. earlandi*, opposite side view; 20 - *Textularia earlandi*, side view; 21 - *Recurvoides turbinatus*, apertural view; 22 - *Reophax scorpiurus*, side view; 23 - *Hormosinella guttifera*, side view; 24 - *Lagenammina difflugiformis*, side view; 25 - *Trochammina globigerineformis*, spiral side view; 26 - *Trochammina ochracea* spiral side view; 27 - *Portatrochammina karica*, spiral side view; 28 - *Deuteramina grahami*, spiral side view; 29, 30 - *Calcispherae*, side view; 31 - *Limacina helicina*, pteropod, side view.

Figure S2. Lithological log and down-core compositional characteristics of core EG-01. The lithofacies refer to the seismic facies (Pedrosa *et al.*, 2011; Lucchi *et al.*, 2013). Magnetic susceptibility after Sagnotti *et al.* (2011) and smectite data after Lucchi *et al.* (2013) are reported. Calcareous nannofossil abundance is expressed as the number of coccoliths 10 mm^{-2} in the slide. Calibrated ages before present (1950) – ka BP – are indicated in red.

Table S1. Number of planktonic foraminifera including number of species and absolute abundance.

Table S2. Number of benthic foraminifera including number of species, absolute abundance and percentage of fragmentation.

Table S3. Number of calcareous nannofossils.

Table S4. Relative abundance of diatoms, including absolute abundance.

Table S5. Radiocarbon dates and ages used to create the age model of the studied cores, from Sagnotti *et al.* (2011) and Lucchi *et al.* (2013, see Fig. 7, p. 319).

Abbreviations. AF, Arctic Front; AW, Atlantic Water; *Chaetoceros* RS, Chaetoceros resting spores; ESC, East Spitsbergen Current; HTM, Holocene Thermal Maximum; IRD, ice-rafted debris; LGM, Last Glacial Maximum; MWP-1a, Meltwater Pulse 1a; PF, Polar Front; TMF, Trough Mouth Fan; WSC, Western Spitsbergen Current; WSG, warm species group YD Younger Dryas.

References

Aagaard-Sørensen S, Husum K, Werner K *et al.* 2014. A Late Glacial-Early Holocene multiproxy record from the eastern Fram Strait, Polar North Atlantic. *Marine Geology* **355**: 15–26.

Abrantes F. 1988. Diatom assemblages as upwelling indicators in surface sediments off Portugal. *Marine Geology* **85**: 15–39.

Andersen C, Koç N, Jennings A *et al.* 2004. Non uniform response of the major surface currents in the Nordic Seas to insolation forcing: implications for the Holocene climate variability. *Paleoceanography* **19**. DOI: 10.1029/2002PA000873

Armand LK, Crosta X, Romero O *et al.* 2005. The biogeography of major diatom taxa in Southern Ocean sediments: 1. *Palaeogeography, Palaeoclimatology, Palaeoecology* **223**: 93–126.

Bárcena MA, Abrantes F. 1998. Evidence of a high-productivity area off the coast of Malaga from studies of diatoms in surface sediments. *Marine Micropaleontology* **35**: 91–103.

Baumann K-H., Matthiessen J. 1992. Variations in surface water mass conditions in the Norwegian Sea: evidence from Holocene coccolith and dinoflagellate cyst assemblages. *Marine Micropaleontology* **20**: 129–146.

Broecker WS, Denton GH, Edwards RL *et al.* 2010. Putting the Younger Dryas cold event into context. *Quaternary Science Reviews* **29**: 1078–1081.

Caralp M. 1989. Abundance of *Bulimina exilis* and *Melonis barleeanum*: relationship to the quality of marine organic matter. *Geo-Marine Letters* **9**: 7–43.

Carbonara K, Mezgec K, Varagona G *et al.* 2016. Palaeoclimatic changes in Kveithola, Svalbard, during the Late Pleistocene deglaciation and Holocene: evidences from microfossil and sedimentary records. *Palaeogeography, Palaeoclimatology, Palaeoecology* **463**: 136–149.

Chauhan T, Rasmussen TL, Noormets R. 2016. Palaeoceanography of the Barents Sea continental margin, north of Nordaustlandet, Svalbard, during the last 74 ka. *Boreas* **45**: 76–99.

Consolaro C, Rasmussen TL, Panieri G. 2018. Palaeoceanographic and environmental changes in the eastern Fram Strait during the last 14,000 years based on benthic and planktonic foraminifera. *Marine Micropaleontology* **139**: 84–101.

Cornelius N, Gooday AJ. 2004. 'Live' (stained) deep-sea benthic foraminiferans in the western Weddell Sea: trends in abundance, diversity and taxonomic composition along a depth transect. *Deep Sea Research Part II: Topical Studies in Oceanography* **51**: 1571–1602.

Darling KF, Kucera M, Kroon D *et al.* 2006. A resolution for the coiling direction paradox in *Neogloboquadrina pachyderma*. *Paleoceanography* **21**: PA2011.

de Kaenel EP, Villa G. 1996. Oligocene-Miocene calcareous nannofossil biostratigraphy and paleoecology from the Iberia Abyssal Plain. *Proceedings of the Ocean Drilling Program* **149**: 79–145.

De Sève MA. 1999. Transfer function between surface sediment diatom assemblages and sea-surface temperature and salinity of the Labrador Sea. *Marine Micropaleontology* **36**: 249–267.

Deschamps P, Durand N, Bard E *et al.* 2012. Ice-sheet collapse and sea-level rise at the Bølling warming 14,600 years ago. *Nature* **483**: 559–564.

Dolven JK, Cortese G, Bjørklund KR. 2002. A high-resolution radiolarian-derived paleotemperature record for the Late Pleistocene-Holocene in the Norwegian Sea. *Paleoceanography* **17**: 1072.

Dylmer CV, Giraudeau J, Eynaud F *et al.* 2013. Northward advection of Atlantic water in the eastern Nordic Seas over the last 3000 yr. *Climate of the Past* **9**: 1505–1518.

Ellison CRW, Chapman MR, Hall IR. 2006. Surface and Deep Ocean interactions during the Cold Climate Event 8200 years ago. *Science* **312**: 1929–1932.

Feyling-Hanssen RW, Jørgensen JA, Knudsen KL *et al.* 1971. Late Quaternary foraminifera from Vendsyssel, Denmark and Sandnes, Norway. *Bulletin of the Geological Society of Denmark* **21**: 67–317.

Flores JA, Sierro FJ, Francés G *et al.* 1997. The last 100,000 years in the western Mediterranean: sea surface water and frontal dynamics as revealed by coccolithophores. *Marine Micropaleontology* **29**: 351–366.

Gard G, Backman J. 1990. Synthesis of arctic and sub-arctic coccolith biochronology and history of North Atlantic Drift Water influx during the last 500.000 years. In *Geological History of the Polar Oceans: Arctic* Versus *Antarctic*, Bleil U, Thiede J (eds). Nato ASI Series **308**: 417–436.

Gooday AJ. 1993. Deep-sea benthic foraminiferal species which exploit phytodetritus: characteristic features and controls on distribution. *Marine Micropaleontology* **22**: 187–205.

Groot DE, Aagaard-Sørensen S, Husum K. 2014. Reconstruction of Atlantic water variability during the Holocene in the western Barents Sea. *Climate of the Past* **10**: 51–62.

Hald M, Korsun S. 1997. Distribution of modern benthic foraminifera from fjords of Svalbard, European Arctic. *Journal of Foraminiferal Research* **27**: 101–122.

Hemleben Ch, Spindler M, Anderson OR. 1989. *Modern Planktonic Foraminifera*. Springer Verlag: Berlin.

Henderiks J, Bollmann J. 2004. The *Gephyrocapsa* sea surface palaeothermometer put to the test: comparison with alkenone and foraminifera proxies off NW Africa. *Marine Micropaleontology* **50**: 161–184.

Husum K, Hald M. 2012. Arctic planktic foraminiferal assemblages: implications for subsurface temperature reconstructions. *Marine Micropaleontology* **96–97**: 38–47 [DOI: 10.1016/j.marmicro.2012.07.001].

Husum K, Hald M, Stein R *et al.* 2015. Recent benthic foraminifera in the Arctic Ocean and Kara Sea continental margin. *Arktos* **1**: 5.

Ishman SE, Foley KM. 1996. Modern benthic foraminifer distribution in the Amerasian Basin, Arctic Ocean. *Micropaleontology* **42**: 206–220.

Jennings AE, Weiner NJ, Helgadottir. 2004. Modern Foraminiferal faunas of the southwestern to northern Iceland shelf: oceanographic and environmental controls. *Journal of Foraminiferal Research* **34**: 180–207.

Jessen SP, Rasmussen TL. 2015. Sortable silt cycles in Svalbard slope sediments 74-0 ka. *Journal of Quaternary Science* **30**: 743–753.

Jessen SP, Rasmussen TL, Nielsen T *et al.* 2010. A new Late Weichselian and Holocene marine chronology for the western Svalbard slope 30,000–0 cal years bp. *Quaternary Science Reviews* **29**: 1301–1312.

Johannessen OM. 1986. Brief overview of the physical oceanography. In *The Nordic Seas*, Hurdle BG (ed.). Springer: New York 103–127.

Junttila J, Aagaard-Sørensen S, Husum K *et al.* 2010. Late Glacial-Holocene clay minerals elucidating glacial history in the SW Barents Sea. *Marine Geology* **276**: 71–85.

Kaufman DS, Ager TA, Anderson NJ. 2004. Holocene thermal maximum in the western Arctic (0-180°W). *Quaternary Science Reviews* **23**: 529–560.

Kemp AES, Pike J, Pearce RB *et al.* 2000. The 'fall dump' — A new perspective on the role of a "shade flora" in the annual cycle of diatom production and export flux. *Deep Sea Research Part II: Topical Studies in Oceanography* **47**: 2129–2154.

Kemp AES, Villareal TA. 2013. High diatom production and export in stratified waters — A potential negative feedback to global warming. *Progress in Oceanography* **119**: 4–23.

Kienast M, Hanebuth TJJ, Pelejero C *et al.* 2003. Synchroneity of meltwater pulse 1a and the Bølling warming: new evidence from the South China Sea. *Geology* **31**: 67–70.

Knies J, Matthiessen J, Vogt C *et al.* 2009. The Plio-Pleistocene glaciation of the Barents Sea-Svalbard region: a new model based on revised chronostratigraphy. *Quaternary Science Reviews* **28**: 812–829

Knudsen KL, Stabell B, Seidenkrantz MS *et al.* 2008. Deglacial and Holocene conditions in northernmost Baffin Bay: sediments, foraminifera, diatoms and stable isotopes. *Boreas* **37**: 346–376.

Koç-Karpuz N, Schrader H. 1990. Surface sediment diatom distribution and Holocene paleotemperature variations in the Greenland, Iceland and Norwegian Sea. *Paleoceanography* **5**: 557–580.

Kohfeld KE, Fairbanks RG, Smith SL *et al.* 1996. *Neogloboquadrina pachyderma* (sinistral coiling) as paleoceanographic tracers in polar oceans: evidence from Northeast Water Polynya plankton tows, sediment traps, and surface sediments. *Paleoceanography* **11**: 679–699.

Korsun S, Hald M. 1998. Modern benthic foraminifera off Novaya Zemlya tidewater glaciers, Russian Arctic. *Arctic and Alpine Research* **30**: 61–77.

Korsun S, Hald M. 2000. Seasonal dynamics of benthic foraminifera in a glacially fed fjord of Svalbard, European Arctic. *Journal of Foraminiferal Research* **30**: 251–271.

Korsun SA, Pogodina IA, Forman SL *et al.* 1995. Recent foraminifera in glaciomarine sediments from three arctic fjords of Novaja Zemlja and Svalbard. *Polar Research* **14**: 15–31.

Klitgaard Kristensen DK, Rasmussen TL, Koç N. 2013. Palaeoceanographic changes in the northern Barents Sea during the last 16 000 years—new constraints on the last deglaciation of the Svalbard-Barents Sea Ice Sheet. *Boreas* **42**: 798–813.

Laberg JS, Vorren TO. 1996. The glacier-fed fan at the mouth of Storfjorden trough, western Barents Sea: a comparative study. *Geologische Rundschau* **85**: 338–349.

Lagoe MB. 1977. Recent benthic foraminifera from the Central Arctic Ocean. *Journal of Foraminiferal Research* **7**: 106–129.

Lagoe MB. 1979. Recent benthonic foraminiferal biofacies in the Arctic Ocean. *Micropaleontology* **25**: 214–224.

Lazar KB, Polyak L. 2016. Pleistocene benthic foraminifers in the Arctic Ocean: implications for sea-ice and circulation history. *Marine Micropaleontology* **126**: 19–30.

Leventer A, Domack EW, Ishman SE *et al.* 1996. Productivity cycles of 200–300 years in the Antarctic Peninsula region: understanding linkages among the sun, atmosphere, oceans, sea ice, and biota. *Geological Society of America Bulletin* **108**: 1626–1644.

Loeng H. 1991. Features of the physical oceanographic conditions of the Barents Sea. *Polar Research* **10**: 5–18.

Lubinski DJ, Polyak L, Forman SL. 2001. Freshwater and Atlantic Water inflows to the deep northern Barents and Kara seas since ca 13 ^{14}C ka: foraminifera and stable isotopes. *Quaternary Science Reviews* **20**: 1851–1879.

Lucchi RG, Camerlenghi A, Rebesco M *et al.* 2013. Postglacial sedimentary processes on the Storfjorden and Kveithola trough mouth fans: significance of extreme glacimarine sedimentation. *Global and Planetary Change* **111**: 309–326.

Lucchi RG, Sagnotti L, Camerlenghi A *et al.* 2015. Marine sedimentary record of meltwater Pulse 1a along the NW Barents Sea continental margin. *Arktos* **1**: 7.

Lutze GF, Thiel H. 1989. Epibenthic foraminifera from elevated microhabitats: *Cibicidoides wuellerstorfi* and *Planulina ariminensis*. *Journal of Foraminiferal Research* **19**: 153–158.

Mackensen A, Sejrup HP, Jansen E. 1985. The distribution of living benthic foraminifera on the continental slope and rise off southwest Norway. *Marine Micropaleontology* **9**: 275–306.

Mangerud J, Gulliksen S. 1975. Apparent Radiocarbon Ages of recent marine shells from Norway, Spitsbergen, and Arctic Canada. *Quaternary Research* **5**: 263–273.

McQuoid MR, Nordberg K. 2003. The diatom *Paralia sulcata* as an environmental indicator species in coastal sediments. *Estuarine, Coastal and Shelf Science* **56**: 339–354.

Murray J. 2006. *Ecology and Applications of Benthic Foraminifera*. Cambridge University Press: Cambridge.

Osterman LE, Poore RZ, Foley KM. 1999. Distribution of benthic foraminifers (> 125 μm) in the surface sediments of the Arctic Ocean. *United States Geological Survey Bulletin* **2164**.

Pedrosa MT, Camerlenghi A, De Mol B *et al.* 2011. Seabed morphology and shallow sedimentary structure of the Storfjorden and Kveithola trough-mouth fans (North West Barents Sea). *Marine Geology* **286**: 65–81.

Pogodina IA. 1999. Distribution of benthonic and planktonic foraminifera in deposits of the Storfjord trough, in the western Barents Sea. Polish Polar Studies. XXVI Polar Symposium, Lublin, June 1999; 203–214.

Polyak L, Best KM, Crawford KA *et al.* 2013. Quaternary history of sea ice in the western Arctic Ocean based on foraminifera. *Quaternary Science Reviews* **79**: 145–156

Polyak L, Korsun S, Febo LA. 2002. Benthic foraminiferal assemblages from the southern Kara Sea, a river-influenced Arctic marine environment. *Journal of Foraminiferal Research* **32**: 252–273.

Rae JWB, Sarnthein M, Foster GL *et al.* 2014. Deep Water formation in the North Pacific and deglacial CO_2 rise. *Paleoceanography* **29**: 645–667.

Rahmstorf S. 2002. Ocean circulation and climate during the past 120,000 years. *Nature* **419**: 207–214.

Rasmussen TL, Thomsen E. 2015. Palaeoceanographic development in Storfjorden, Svalbard, during the deglaciation and Holocene: evidence from benthic foraminiferal records. *Boreas* **44**: 24–44.

Rasmussen TL, Thomsen E, Skirbekk K *et al.* 2014. Spatial and temporal distribution of Holocene temperature maxima in the northern Nordic seas: interplay of Atlantic-, Arctic- and polar water masses. *Quaternary Science Reviews* **92**: 280–291.

Rasmussen TL, Thomsen E, Ślubowska MA *et al.* 2007. Paleoceanographic evolution of the SW Svalbard margin (76°N) since 20,000 ^{14}C yr bp. *Quaternary Research* **67**: 100–114.

Renssen H, Seppä H, Crosta X *et al.* 2012. Global characterization of the Holocene Thermal Maximum. *Quaternary Science Reviews* **48**: 7–19.

Renssen H, Seppä H, Heiri O *et al.* 2009. The spatial and temporal complexity of the Holocene thermal maximum. *Nature Geoscience* **2**: 411–414.

Risebrobakken B, Dokken T, Smedsrud LH *et al.* 2011. Early Holocene temperature variability in the Nordic Seas: the role of oceanic heat advection versus changes in orbital forcing. *Paleoceanography* **26**: PA4206.

Rohling EJ, Pälike H. 2005. Centennial-scale climate cooling with a sudden cold event around 8,200 years ago. *Nature* **434**: 975–979.

Roth PH, Coulbourn WT. 1982. Floral and solution patterns of coccoliths in surface sediments of the North Pacific. *Marine Micropaleontology* **7**: 1–52.

Sagnotti L, Macrì P, Lucchi RG *et al.* 2011. A Holocene paleosecular variation record from the northwestern Barents Sea continental margin. *Geochemistry, Geophysics, Geosystems* **12**: Q11Z33.

Saloranta TM, Svendsen H. 2001. Across the Arctic front west of Spitsbergen: high-resolution CTD sections from 1998–2000. *Polar Research* **20**: 177–184.

Samtleben C, Bickert T. 1990. Coccoliths in sediment traps from the Norwegian Sea. *Marine Micropaleontology* **16**: 39–64.

Samtleben C, Schäfer P, Andruleit H *et al.* 1995. Plankton in the Norwegian-Greenland Sea: from living communities to sediment assemblages-an actualistic approach. *Geologische Rundschau* **84**: 108–136.

Sarnthein M. 2011. Paleoclimate. Northern meltwater pulses, CO_2, and changes in Atlantic convection. *Science* **331**: 156–158.

Sarnthein M, Van Kreveld S, Erlenkeuser H *et al.* 2003. Centennial-to-millennial-scale periodicities of Holocene climate and sediment injections off the western Barents shelf, 75°N. *Boreas* **32**: 447–461.

Schauer U, Fahrbach E, Osterhus S. 2004. Arctic warming through the Fram Strait: oceanic heat transport from 3 years of measurements. *Journal of Geophysical Research* **109**: C06026.

Schiebel R, Hemleben C. 2000. Interannual variability of planktic foraminiferal populations and test flux in the eastern North Atlantic Ocean (JGOFS). *Deep Sea Research Part II: Topical Studies in Oceanography* **47**: 1809–1852.

Schiebel R, Waniek J, Bork M *et al.* 2001. Planktic foraminiferal production stimulated by chlorophyll redistribution and entrainment of nutrients. *Deep Sea Research Part I: Oceanographic Research Papers* **48**: 721–740.

Schrader HJ, Gersonde R. 1978. Diatoms and silicoflagellates. In *Micropaleontological Counting Methods and Techniques: an Exercise of an Eight Metres Section of the Lower Pliocene of Cap Rossello, Sicily,* Zachariasse WJ *et al.* (eds). *Utrecht Micropaleontological Bulletin* **17**: 129–176.

Schröder-Adams CJ, Cole FE, Medioli FS *et al.* 1990. Recent Arctic shelf foraminifera: seasonally ice covered areas vs. perennially ice covered areas. *Journal of Foraminiferal Research* **20**: 8–36.

Scott DB, Vilks G. 1991. Benthic foraminifera in the surface sediments of the deep-sea Arctic Ocean. *Journal of Foraminiferal Research* **21**: 20–38.

Sejrup H-P, Fjaeran T, Hald M *et al.* 1981. Benthonic foraminifera in surface samples from the Norwegian continental margin between 62 degrees N and 65 degrees N. *Journal of Foraminiferal Research* **11**: 277–295.

Ślubowska MA, Koç N, Rasmussen TL *et al.* 2005. Changes in the flow of Atlantic water into the Arctic Ocean since the last deglaciation: evidence from the northern Svalbard continental margin, 80°N. *Paleoceanography* **20**. DOI: 10.1029/2005P A001141

Ślubowska-Woldengen M, Koç N, Rasmussen TL *et al.* 2008. Time-slice reconstructions of ocean circulation changes on the continental shelf in the Nordic and Barents Seas during the last 16,000 cal yr B.P. *Quaternary Science Reviews* **27**: 1476–1492.

Ślubowska-Woldengen M, Rasmussen TL, Koç N *et al.* 2007. Advection of Atlantic Water to the western and northern Svalbard shelf since 17,500 cal yr bp. *Quaternary Science Reviews* **26**: 463–478.

Stabell B. 1986. A diatom maximum horizon in upper Quaternary deposits. *Geologische Rundschau* **75**: 175–184.

Steinsund PI. 1994. *Benthic foraminifera in surface sediments of the Barents and Kara seas: modern and late Quaternary applications*. PhD Thesis, University of Tromso.

Stuiver M, Reimer PJ. 1993. Extended ^{14}C data base and revised CALIB 3.0 ^{14}C age calibration program *Radiocarbon* **35**: 215–230.

Thomas E, Booth L, Maslin M *et al.* 1995. Northeastern Atlantic benthic foraminifera during the last 45,000 years: changes in productivity seen from the bottom up. *Paleoceanography* **10**: 545–562.

Thornalley DJ, Bauch HA, Gebbie G *et al.* 2015. A warm and poorly ventilated deep Arctic Mediterranean during the last glacial period. *Science* **349**: 706–710.

Tomas CR. 1997. *Identifying Marine Phytoplankton*. Academic Press: New York.

Villa G, Persico D, Wise SW *et al.* 2012. Calcareous nannofossil evidence for Marine Isotope Stage 31 (1Ma) in Core AND-1B, ANDRILL McMurdo Ice Shelf Project (Antarctica). *Global and Planetary Change* **96–97**: 75–86.

Wells P, Okada H. 1997. Response of nannoplankton to major changes in sea-surface temperature and movements of hydrological fronts over Site DSDP 594 (south Chatham Rise, southeastern New Zealand), during the last 130 kyr. *Marine Micropaleontology* **32**: 341–363.

Werner K, Müller J, Husum K *et al.* 2016. Holocene sea subsurface and surface water masses in the Fram Strait-comparisons of temperature and sea-ice reconstructions. *Quaternary Science Reviews* **147**: 194–209.

Werner K, Spielhagen RF, Bauch D *et al.* 2013. Atlantic Water advection versus sea-ice advances in the eastern Fram Strait during the last 9 ka: multiproxy evidence for a two-phase Holocene. *Paleoceanography* **28**: 283–295.

Williams KM. 1986. Recent Arctic marine diatom assemblages from bottom sediments in Baffin Bay and Davis Strait. *Marine Micropaleontology* **10**: 327–341.

Wollenburg JE, Knies J, Mackensen A. 2004. High-resolution paleoproductivity fluctuations during the past 24 kyr as indicated by benthic foraminifera in the marginal Arctic

Ocean. *Palaeogeography, Palaeoclimatology, Palaeoecology* **204**: 209–238.

Wollenburg JE, Kuhnt W. 2000. The response of benthic foraminifers to carbon flux and primary production in the Arctic Ocean. *Marine Micropaleontology* **40**: 189–231.

Wollenburg JE, Mackensen A. 1998. Living benthic foraminifers from the central Arctic Ocean: faunal composition, standing stock and diversity. *Marine Micropaleontology* **34**: 153–185.

Wollenburg JE, Mackensen A. 2009. The ecology and distribution of benthic foraminifera at the Håkon Mosby mud volcano (SW Barents Sea slope). *Deep Sea Research Part I: Oceanographic Research Papers* **56**: 1336–1370.

Zamelczyk K, Rasmussen TL, Husum K *et al*. 2012. Paleoceanographic changes and calcium carbonate dissolution in the central Fram Strait during the last 20 ka. *Quaternary Research* **78**: 405–416.